energies

MDPI

Article

Degradation of Soft Epoxy Resin for Cable Penetrations Induced by Simulated Severe Accidents

Yoshimichi Ohki [1,2,*], Hiroyuki Ishii [2] and Naoshi Hirai [1]

[1] Research Institute for Materials Science and Technology, Waseda University, 2-8-26 Nishiwaseda, Shinjuku-ku, Tokyo 169-0051, Japan; nhirai@aoni.waseda.jp
[2] Department of Electrical Engineering and Bioscience, Waseda University, 3-4-1 Ohkubo, Shinjuku-ku, Tokyo 169-8555, Japan; keyofthetwilight@suou.waseda.jp
* Correspondence: yohki@waseda.jp

Abstract: To obtain the knowledge that contributes to the safer operation of nuclear power plants and their prompt recovery and termination in the event of an accident, soft epoxy resins with rubber-based additives—used as insulators and airtight sealants in electrical penetrations in nuclear power plants—were aged under several simulated severe accident environments with different conditions of heat, gamma rays, and exposure to superheated steam containing no oxygen. Then, changes in structural, dynamic mechanical, mechanical, and dielectric properties were examined. It has been found that this resin becomes hard as a result of cross-linking if aged by irradiation with gamma rays. Since the cross-linking slows down the molecular motions, the glass transition temperature increases, whereas the dielectric permittivity and the dielectric loss factor decrease unless the steam penetrates the sample. Although the sample melts and disappears if directly exposed to superheated steam at 171 °C or 200 °C, the irradiation with gamma rays conducted prior to the steam exposure can mitigate the hydrolysis induced by the steam. Although the soft epoxy resin shows drastic changes in various properties, its properties after the aging approach or exceed the corresponding ones of the non-degraded ordinary hard epoxy resin. Therefore, it seems that using soft epoxy resin according to its purposes would not be a problem.

Keywords: nuclear power plant; steam exposure; aging; gamma rays; electrical insulation; sealant

check for updates

Citation: Ohki, Y.; Ishii, H.; Hirai, N. Degradation of Soft Epoxy Resin for Cable Penetrations Induced by Simulated Severe Accidents. *Energies* **2021**, *14*, 6932. https://doi.org/10.3390/en14216932

Academic Editor: Simone Vincenzo Suraci

Received: 27 September 2021
Accepted: 19 October 2021
Published: 21 October 2021

Publisher's Note: MDPI stays neutral with regard to jurisdictional claims in published maps and institutional affiliations.

Copyright: © 2021 by the authors. Licensee MDPI, Basel, Switzerland. This article is an open access article distributed under the terms and conditions of the Creative Commons Attribution (CC BY) license (https://creativecommons.org/licenses/by/4.0/).

1. Introduction

Epoxy resin is widely used in industries and ordinary households as adhesives and electrical insulating materials because of its excellent heat resistance, electrical insulating properties, and durability [1,2]. On the other hand, when epoxy resin alone has a weak point, various additives or fillers are added to overcome such disadvantages while retaining its excellent properties [1,2]. As a reflection of the importance of epoxy resin with or without fillers, much research has been conducted continuously and vigorously on its many aspects since it began to be utilized in industry [1–8].

The present study deals with epoxy resin being used as airtight sealants in electrical penetrations for cables in nuclear power plants. This material needs good electrical insulating performance as it is expected to work as electrical insulating materials for electric conductors penetrating through the electrical penetrations. It also needs excellent airtightness because of its other vital role in preventing any possible leak of radioactive substances from reactor containment vessels [9,10]. However, some manufacturer of nuclear power apparatus considers that ordinary epoxy resin alone might be too hard for sealants. For this reason, a rubber-based additive is added to epoxy resin, which is called soft epoxy resin, to increase its softness and toughness [11,12].

Due to their function, many electrical penetrations are responsible for ensuring the safety and airtightness of electrical systems in a nuclear power plant not only during its normal operation, but also during a severe accident that might occur on the last day

of its operation [9,10]. Although ordinary hard epoxy resin is mostly used in Japanese pressurized water nuclear power plants, the soft epoxy resin is used in many boiling water nuclear power plants, at least in Japan [11,12]. Therefore, to further improve the safe operation of nuclear power generation and its prompt recovery and termination in an event of an accident, it is of prime importance to confirm the soundness of soft epoxy resin in a possible severe accident occurring in a nuclear power plant by conducting experiments in an environment that simulates the severe accident [11,12].

It is difficult and expensive, especially for researchers in academia, to obtain the same resins as those used in nuclear power plants. It is also difficult to realize an environment that simulates severe accidents. Moreover, research conducted by industries for designing and constructing nuclear power plants has been reported seldom in scientific journals. For these various reasons, almost no academic papers have been reported on the degradation of soft epoxy resin to our best knowledge. Therefore, research on the above topic cannot be fruitful unless it is performed systematically in the form of a large-scale joint research project at least composed of a governmental body and academia with the intention of making its outcomes open to the public. With this view, we have been conducting a series of research projects entrusted by the Secretariat of Nuclear Regulation Authority in Japan with other research organizations. We have, so far, published many papers on the outcomes of the projects such as those listed in the References section of this paper [12–21].

Recently, the importance of research on electrical insulating materials used in cables and their penetrations in nuclear plants, funded by large-scale projects, has also been realized in other countries [22–25]. A project called "European Tools and Methodologies for an efficient ageing management of nuclear power plant Cables", known by its abbreviation TeaM Cables and funded by the Euratom Research and Training Programme, is a typical example of such projects [26].

In one of our such papers [12], we aged samples of soft and hard epoxy resins by giving them heat treatment and gamma-ray irradiation simultaneously that simulated an accelerated operation environment of a nuclear power plant. Then, we compared the changes induced in thermal, mechanical, and dielectric properties between the two epoxy resins. However, no steam exposure was given to the samples in that research.

Regarding the above, in this study, gamma-ray irradiation at a relatively low dose rate under a thermal cycle to simulate an accelerated environment during the normal operation and gamma-ray irradiation at a high dose rate at room temperature to simulate a severe accident—together with subsequent steam exposure that also simulated a severe accident—were applied to soft epoxy resin to investigate the changes induced in various characteristics and consider the governing degradation mechanisms.

2. Materials and Methods

As mentioned above, soft epoxy resin with a rubber-based additive provided by a Japanese supplier of electrical goods for nuclear power plants was used as samples. It was of the same quality as the one used as sealants to make electrical penetrations airtight in many boiling water nuclear power plants in Japan. We found, from instrumental analyses, that the epoxy resin was bisphenol F type and that novolac phenol resin was used as a curing agent, while polybromobisphenol A and Sb_2O_3 were used as flame retardants. However, further information on the rubber-based additive, curing conditions of epoxy resin, etc., is unknown.

Samples of the shape of a sheet, about 1.0 mm thick, with a size suitable to each measurement, were used unless otherwise stated. The thermal cycle shown in Figure 1 was repeated 40 times as an aging procedure to simulate the operation equivalent to 40 years for this epoxy resin [27]. Namely, ^{60}Co gamma rays were irradiated at a dose rate of 100 Gy/h for 960 h at 100 °C and another 960 h at temperatures other than 100 °C. However, since the defined accelerated aging period is 1296 h for the dose rate of 100 Gy/h at 100 °C, additional irradiation for 336 h was added. Here, this aging procedure is referred to as 'thermal cycle C'.

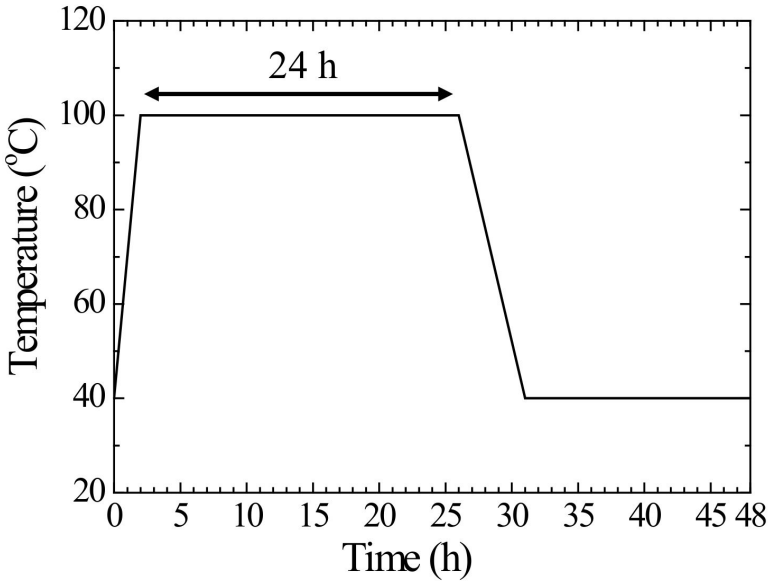


Figure 1. Temperature profile of thermal cycle C simulating the aging during the normal operation period.

In the event of a possible severe accident, radiation and water steam will be exposed at the same time. However, since it is difficult to simulate the above exactly, high dose-rate irradiation and exposure of water steam were given separately to simulate a severe accident. For the high dose-rate irradiation, gamma rays were irradiated at room temperature at a dose rate of 5 kGy/h for 140 h when cycle C had been given in advance, but for 160 h otherwise. The resultant total dose of gamma rays is 930 or 800 kGy, depending on with or without thermal cycle C. Hereafter, this high dose-rate irradiation at room temperature will be referred to as R. When this irradiation R was given after the thermal cycle C, the combined process will be referred to as CR.

The exposure of water steam was conducted in two ways. Firstly, superheated steam containing no air or oxygen was exposed to the sample for 168 h under a pressure of 0.64 MPaG at 171 °C. This process is called medium-temperature and medium-pressure steam exposure S_m. Secondly, the superheated steam was exposed for 168 h under a pressure of 0.90 MPaG at 200 °C, which is called high-temperature and high-pressure steam exposure S_h. The last letter G in 0.90 MPaG means that the pressure is higher than the outside ambiance by 0.90 MPa.

Here, the above aging conditions were adopted according to the reports [27–30] compiled based on the achievements of past research projects entrusted by the Secretariat of Nuclear Regulation Authority in Japan and its preceding organization. In short, C corresponds to the accelerated irradiation to simulate the normal operation period of a nuclear power plant, and R simulates the irradiation during a design-basis accident, while S_m and S_h simulate the steam exposure conditions that would encounter during severe accidents. Thermal cycle C, high dose-rate irradiation R, and steam exposure S_m or S_h were applied alone or in this order. By this, a total of 12 types of samples listed in Table 1—including the undegraded pristine sample P—were prepared. Here, each sample is called by the treatment(s) given to it.

Table 1. Samples and aging conditions of epoxy.

Name	Irradiation			Steam Exposure			Symbol
	Temp. (°C)	Total Dose (kGy)	Dose Rate (kGy/h)	Temp. (°C)	Pressure (MPaG)	Duration (h)	
P	–	–	–	–		–	●
C	100_{max}	230	0.1	–		–	△
R	25	800	5	–		–	□
CR	$100_{max} \geq 25$	930	$0.1 \geq 5$	–		–	◇
S_m	–	–	–	171	0.64	168	○
S_h	–	–	–	200	0.90	168	
CS_m	100_{max}	230	0.1	171	0.64	168	▲
CS_h	100_{max}	230	0.1	200	0.90	168	▲
RS_m	25	800	5	171	0.64	168	■
RS_h	25	800	5	200	0.90	168	■
CRS_m	$100_{max} \geq 25$	930	$0.1 \geq 5$	171	0.64	168	◆
CRS_h	$100_{max} \geq 25$	930	$0.1 \geq 5$	200	0.90	168	◆

Note: 100_{max} means that the temperature was changed according to the thermal cycle shown in Figure 1.

To investigate the mechanical properties, a sample sheet cut into the shape of about $10 \times 5 \times 1$ mm^3, based on a Japanese industrial standard [31], was served to dynamic mechanical analysis (DMA, DMA 242 E Artemis, Netzsch). The complex elastic modulus or its real part E' and imaginary part E'' were measured at a vibrational frequency of 10 Hz while raising and lowering the sample temperature at rates of ±5 °C/min. Here, in our previous research [12], we found that variations in thermal parameters like glass transition temperature (T_g) associated with degradation were much more easily measurable by DMA than by differential scanning calorimetry (DSC) in soft epoxy resin. This is the reason for not using more general DSC.

Next, for each sample, the elongation at break (EAB) and the tensile strength (TS) were measured for five dumbbell-shaped test pieces, specified by a Japanese industrial standard [32], with a tensile speed of 500 mm/min by a universal tester (5565 type, Instron).

Furthermore, the indenter modulus (IM) was measured using an IM-INSS III (Tobusa Systems) indenter by pushing a metal needle with a tip diameter of 0.79 mm into the sample surface at a speed of 0.080 mm/s. Here, IM is defined as the load in N, averaged in a load range from 1 to 4 N, necessary to push the needle further by 1.0 mm [33]. The measurement was performed six times by changing the measurement position on the sample surface.

In addition, the complex permittivity was measured using a sample sheet cut into a square of 4×4 cm^2 with an aluminum circular electrode of a 20-mm diameter on each surface attached with silicone oil. The measurement was conducted at room temperature of about 20 °C in vacuum with ac voltages of 3 V_{rms} in a frequency range from 10^{-2}–10^5 Hz using an impedance analyzer (SI126096W, Solartron).

Furthermore, Fourier transform mid-infrared absorption (FT-MIR) spectra were obtained in the attenuated total reflection (ATR) mode using an FT/IR-4200 spectrometer (JASCO).

3. Results

3.1. Disappearance of Samples by Hydrolysis

First, when the pristine undegraded sample P was directly exposed to superheated water steam at 171 °C or 200 °C, it disappeared. In other words, the superheated water steam causes hydrolysis and decomposes and melts the soft epoxy resin so severely that we cannot have samples S_m and S_h, regardless of the condition of steam exposure. On the other hand, all other steam-exposed samples, such as samples CS_h and RS_h or those

previously irradiated with gamma rays, could be used for various measurements even after the high-temperature and high-pressure steam exposure. Namely, the prior gamma-ray irradiation conducted properly can mitigate the hydrolysis induced by successive water steam. According to our previous paper [14], the hydrolysis of silicone rubber is suppressed if gamma rays were irradiated beforehand. The above important fact clearly shows that the mitigation of material decomposition occurs similarly in soft epoxy resin and silicone rubber if these samples were irradiated with gamma rays beforehand.

3.2. Dynamic Mechanical Analysis

3.2.1. DMA Spectra

Figure 2 shows the DMA spectra acquired for each sample, representing the changes in storage elastic modulus E' and the loss elastic modulus E'' as a function of measurement temperature, in addition to tan δ defined as E''/E'. A logarithmic scale is used for E'. Here, except for sample P, the samples before and after the exposure to water steam are compared on single graphs to help understand the effects of steam exposure. In principle, if we think of the mechanism of the glass transition, the peak temperature of E'' should be regarded as T_g. In case that the peak temperature of E'' is ambiguous and difficult to determine for any reason, the inflection point of the E' curve should be regarded as T_g. However, the peak temperature of tan δ is often considered as T_g [34,35]. The reason for this is likely that the change in tan δ represented by E''/E' appears obviously even when E'' and E' are too small to recognize their changes on a graph. Since the definition of T_g by the tan δ curve is more obvious, we adopted this method.

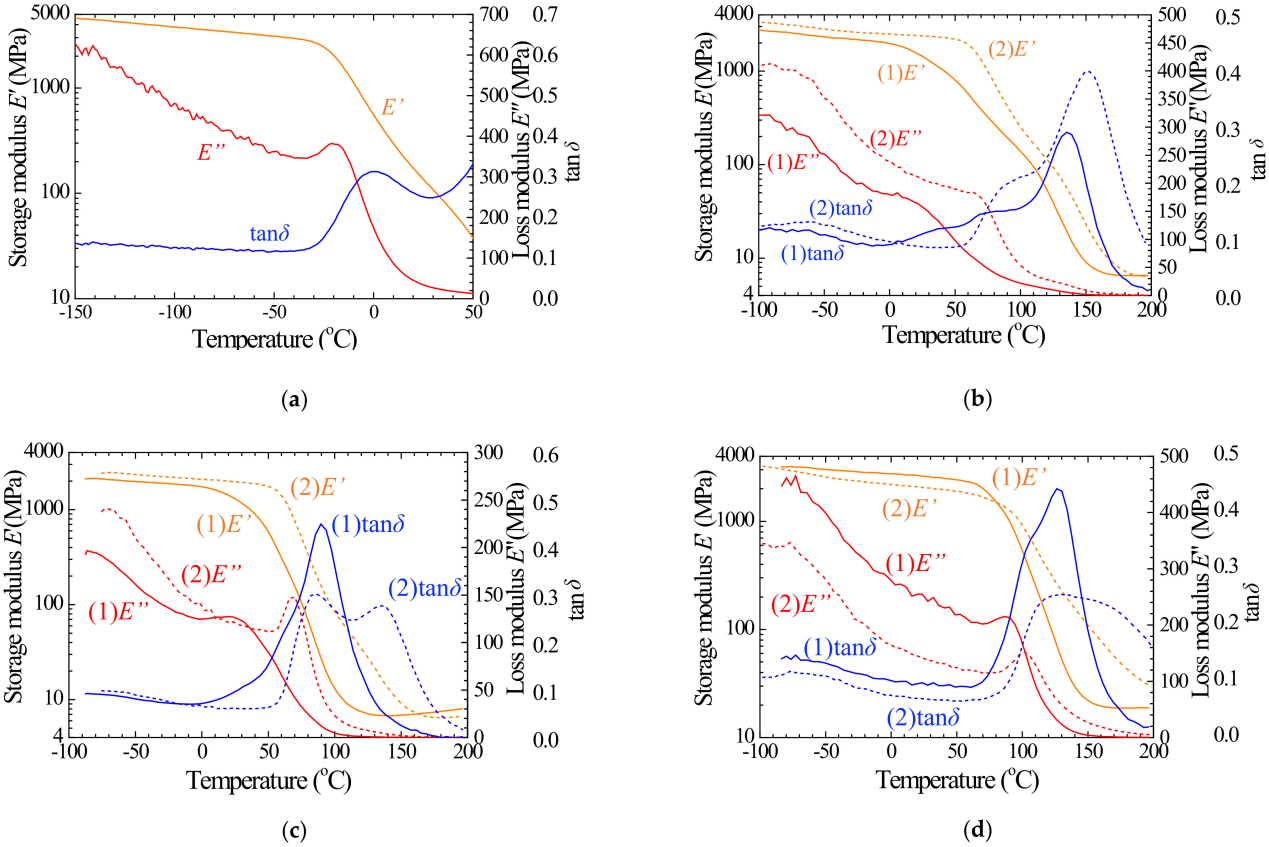


Figure 2. E', E'', and tan δ measured by DMA as a function of measurement temperature. Refer to Table 1 for the aging condition of each sample. (**a**) Unaged sample P, (**b**) Samples C (1) and CSm (2), (**c**) Samples R (1) and RS_m (2), (**d**) Samples CR (1) and CRSm (2). The numbers in parentheses (1) and (2) next to curves indicate the corresponding samples.

The peak of tan δ appears at a temperature away from the shoulder of E'' in samples C and CS_m in Figure 2b. Two peaks are seen in tan δ in sample RS_m in Figure 2c, indicating that two types of glass transition and the associated T_g's are present. Hereafter, when two peaks that should be regarded as T_g are seen, those at the higher and lower temperatures are referred to as T_{gh} and T_{gl}, respectively. If we think of the temperatures alone, it seems that T_{gh} at 136 °C is due to the epoxy resin, while T_{gl} at 85 °C is due to the rubber-based additives.

3.2.2. Glass Transition Temperature

Figure 3 shows T_{gl} measured in each sample as a function of thermal aging time at 100, 171, or 200 °C. Here, if we take samples C and RS_m as examples, sample C was exposed to heat at 100 °C for 1296 h during the thermal cycle C as mentioned above, while sample RS_m was exposed to heat at 171 °C for 168 h during the steam exposure S_m. The above period of 1296 h or 168 h is shown on the abscissa of Figure 3, irrespective of such a difference in thermal aging temperature. In Figure 3, changes in T_{gl} similarly measured in our previous research [12] by DMA for the samples aged concurrently with heat at 100 °C and gamma-ray irradiation at 100 Gy/h are also shown. As the aging time increases, T_{gl} increases almost monotonically, but with a slight exception that T_{gl} in sample RS_m decreases a little compared to sample R.

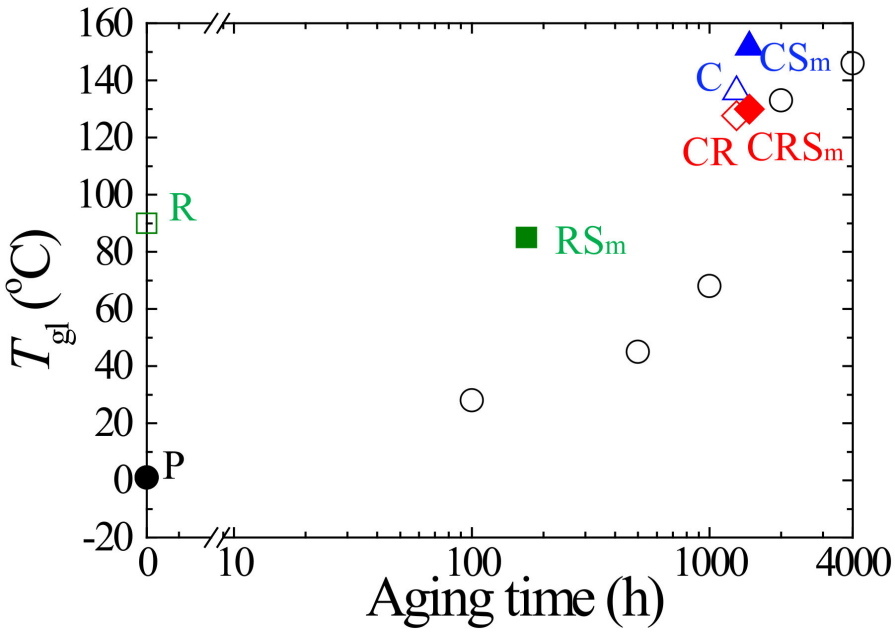


Figure 3. T_{gl} as a function of thermal aging time; P(●), C(△), CS_m(▲), R(□), RS_m(■), CR(◇), and CRS_m(◆); ○: Data measured in the samples aged concurrently with heat at 100 °C and gamma-ray irradiation at 100 Gy/h, reported in our previous paper [12].

3.2.3. Storage and Loss Moduli

Furthermore, Figure 4 shows E' and E'' measured at 20 °C. The values of E' and E'' measured for the samples aged concurrently with heat at 100 °C and gamma-ray irradiation at 100 Gy/h, reported in our previous paper [12], are also shown. With the increase in aging time or apparent progress of degradation, E' and E'' increase monotonically, but they are lower in sample CRS_m than in sample CR.

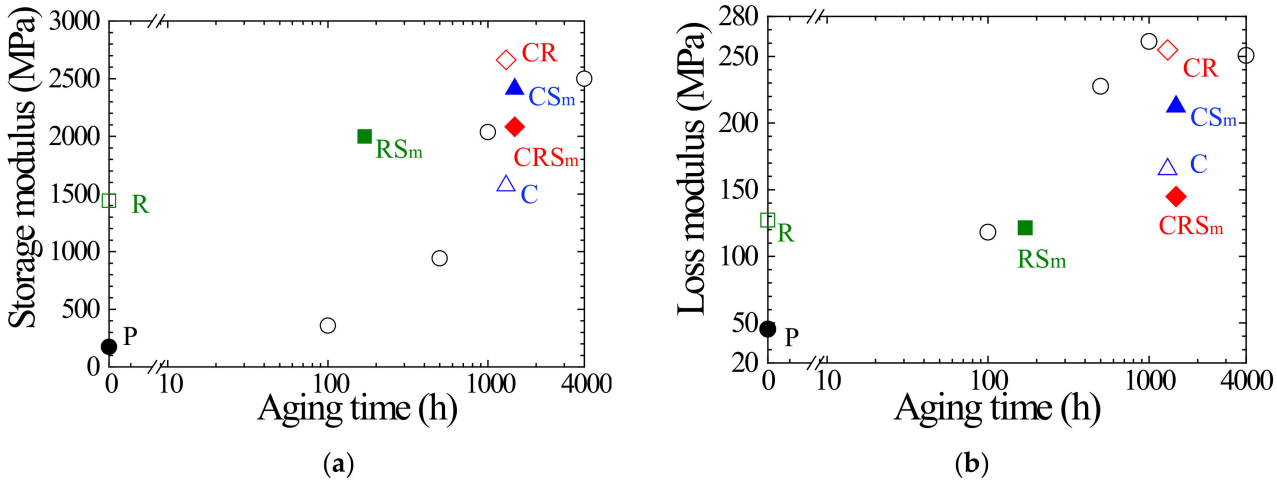


Figure 4. Storage modulus E' (**a**) and loss modulus E'' (**b**) as a function of thermal aging time. Refer to Table 1 and Figure 3 for the sample symbols; ○: Data measured in the samples aged concurrently with heat at 100 °C and gamma-ray irradiation at 100 Gy/h, reported in our previous paper [12].

3.3. Mechanical Properties

3.3.1. Tensile Tests

Next, changes in EAB and TS acquired from the tensile tests conducted for various samples are shown in Figure 5. Note that both EAB and TS were set to 0 for the samples S_m and S_h exposed to the water steam that melted and disappeared. The reduction of EAB observed in each sample from the pristine sample P is as follows: steam exposure (S_m and S_h) > irradiation R > thermal cycle C. On the other hand, if we think of the effects of steam exposure on samples P, R, and C by comparing the values of EAB before and after the steam exposure in each sample, it becomes sample P > sample C > sample CR ≥ sample R. That is, the reduction in EAB in sample S_m (or S_h) from sample P is the most significant and the least significant in sample RS_m from sample R. On the other hand, TS increases in samples C and R compared to sample P, while it decreases by the subsequent steam exposure. However, TS increases in sample RS_m exposed to medium-temperature and medium-pressure steam compared to sample R.

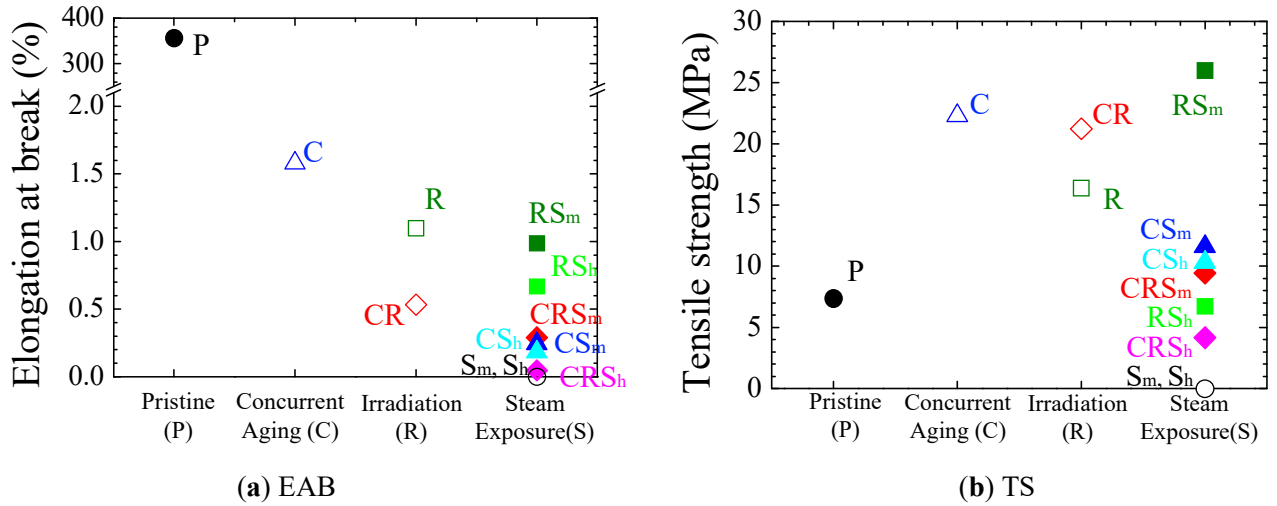


Figure 5. EAB (**a**) and TS (**b**) as a function of aging condition; P(●), C(△), CS_m(▲), CS_h(▲), R(□), RS_m(■), RS_h(■), CR(◇), CRS_m(◆), CRS_h(◆), S_m (○), and S_h (○).

3.3.2. Indenter Modulus

Furthermore, Figure 6 shows the average and the standard deviation of IM. The average value of IM becomes higher in samples C and R compared to sample P. Furthermore, the average value of IM generally becomes lower and the standard deviation becomes wider by the exposure to water steam, although there are several exceptions such as the higher averages in samples RS_m and RS_h compared to sample R.

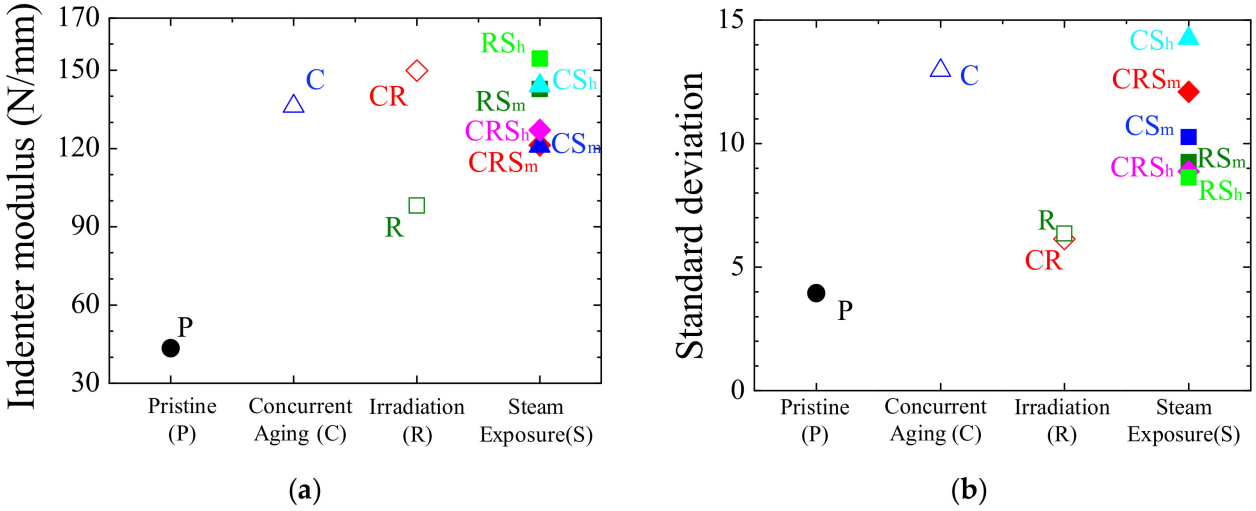


Figure 6. IM as a function of aging condition. Refer to Table 1 and Figure 5 for the sample symbols. (**a**) Average of indenter modulus, (**b**) Standard deviation.

3.4. Dielectric Properties

In addition, the values of the relative permittivity ε_r' and the dielectric loss factor ε_r'' at 50 Hz measured at room temperature are shown in Figure 7 as a function of the aging condition. In most samples, ε_r' and ε_r'' significantly decrease compared to sample P. However, only in sample CRS_h, they become higher drastically, probably due to the permeation of water steam into the samples.

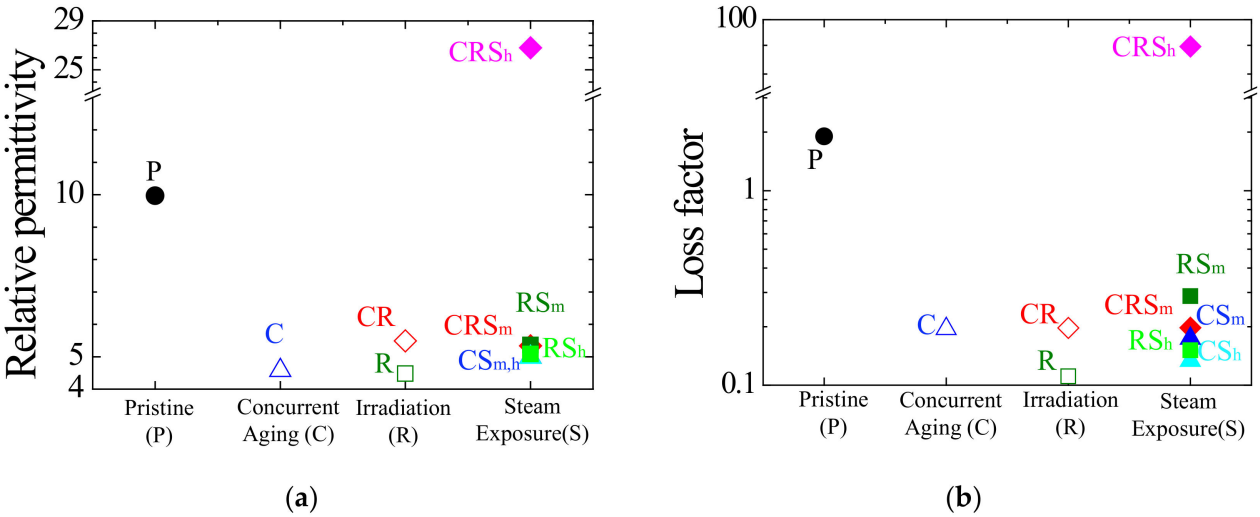


Figure 7. Aging-condition dependence of relative permittivity ε_r' (**a**) and loss factor ε_r'' (**b**). Refer to Table 1 and Figure 5 for the sample symbols. (**a**) Relative permittivity ε_r', (**b**) Loss factor ε_r''.

3.5. Fourier Transform Mid-Infrared Absorption Spectra

Finally, Figure 8 shows the FT-MIR spectra as important parameters indicating possible structural changes induced by various aging processes. Note that the spectral intensity measured by ATR may vary significantly, depending on the contact condition between the sample surface and a prism for the measurement, which is ZnSe in this research. Therefore, the absorption intensity should be normalized by that of a stable reference peak. In this regard, the absorption intensity was normalized by that of the flame retardant Sb_2O_3 appearing around 738 cm^{-1}.

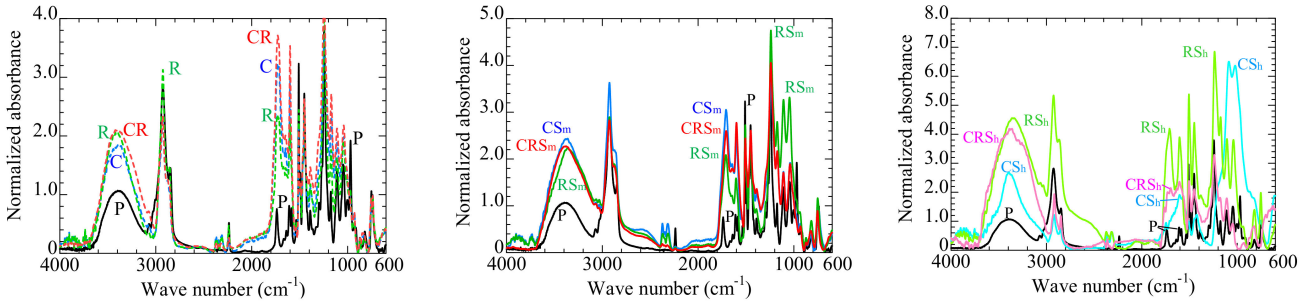


Figure 8. FT-MIR spectra measured in various samples. (**a**) aged without the steam exposure; P: pristine (—), C: thermal cycles (—), R: high-dose-rate radiation (—), CR: thermal cycles and high-dose-rate radiation (—). (**b**) aged with steam exposure S_m; P: —, CS_m: —, RS_m: —, CRS_m: —. (**c**) aged with steam exposure S_h; P: —, CS_h: —, RS_h: —, CRS_h: —.

Here, we pay attention to the absorption due to C=O groups formed by the oxidation at 1740 cm^{-1}. Figure 9 shows the sample-dependent intensity of such peak-separated and integrated absorption around 1740 cm^{-1}. It is clearly shown that the thermal cycle C and the high dose-rate irradiation at room temperature R increase the integrated absorption due to C=O from sample P, whereas the medium-temperature and medium-pressure steam exposure S_m given to the samples C, R, and CR hardly changes the integrated absorption. However, the high-temperature and high-pressure steam exposure S_h decreases the integrated absorption, especially significantly when it was given to samples C and CR.

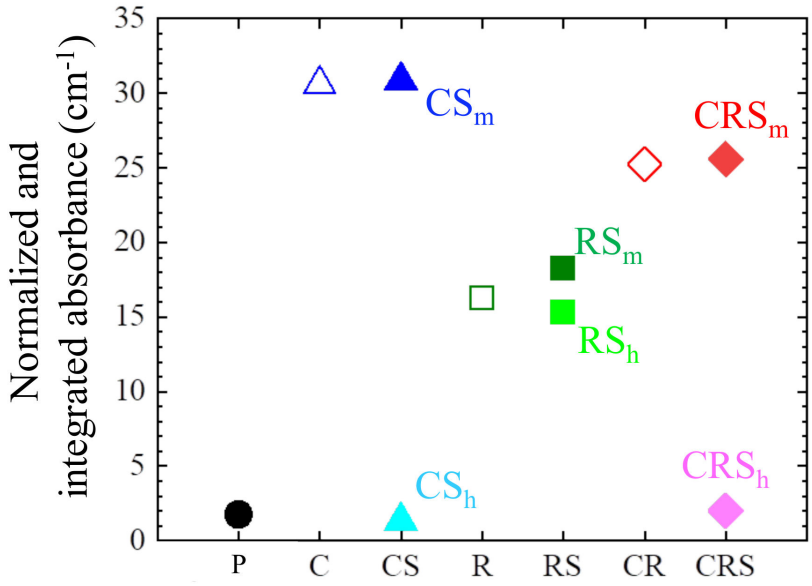


Figure 9. Normalized and integrated absorbance due to carbonyl groups (1740 cm^{-1}). Refer to Table 1 and Figure 5 for the sample symbols.

4. Discussion

4.1. Aging Induced Structural Changes

First, as shown in Figure 9, the absorption due to C=O becomes higher in samples C, R, and CR than sample P, indicating that the soft epoxy resin is oxidized when it was irradiated with gamma rays. In more detail, the normalized intensity is the highest in sample C with a small difference in CR, which is followed by R. Here, the total gamma-ray doses irradiated to C, R, and CR are respectively 230, 800, and 930 kGy as listed in Table 1. This means that carbonyl groups should appear much more abundantly in sample C if we compare their quantities at the same irradiation dose. Since sample C was irradiated with gamma rays during the repeated thermal cycles with the maximum irradiation temperature of 100 °C under the low dose rate of 0.1 kGy/h, the diffusion of oxygen into the sample bulk was thermally activated to oxidize the sample sufficiently. This is a kind of dose-rate effect of oxidation [36,37].

On the other hand, it is most likely that the oxygen inside the sample would become insufficient soon after the initiation of the irradiation R due to its high dose rate and low temperature. In this regard, the oxidation is suppressed and cross-linking is promoted in sample R, which is a phenomenon often seen in organic polymers [15,17].

The fact that the comparatively milder steam exposure S_m gives no clear effects on the C=O abundance in the samples CS_m, RS_m, and CRS_m, as shown in Figure 9, is natural in one sense since the superheated steam used for the steam exposure had no air or oxygen. However, this fact has an important meaning when we think of the fact that sample S_m melted and disappeared. That is, when soft epoxy resin was irradiated beforehand by gamma rays irrespective of the conditions of C, R, and CR, the sample seems to be able to withstand the medium-temperature and medium-pressure steam exposure S_m. In contrast, the C=O abundance exhibits an obvious decrease in the samples CS_h and CRS_h after the high-temperature and high-pressure steam exposure S_h, whereas the above abundance hardly changes in sample RS_h. This means that soft epoxy resin can withstand the severe steam exposure S_h when it was pre-irradiated by gamma rays only under the condition R. As mentioned above, the non-irradiated soft epoxy resin melts and disappears when it is exposed to superheated steam S_m or S_h. This indicates that chemical bonds in the resin are cut by hydrolysis induced by the steam exposure. On the other hand, if the sample is cross-linked and its chemical bonds and resultant structure become three-dimensional, it should make the resin harder and more robust. Such a three-dimensional hard structure should decelerate the penetration of water molecules into the sample bulk and make the chemical bonds more robust.

4.2. Dynamic Mechanical Analysis

Next, we pay attention to the changes in T_{gl}, shown in Figure 3. First, T_{gl} measured in the samples irradiated with gamma rays with the dose rate of 100 Gy/h at 100 °C exhibits a monotonic increase as the aging time increases [12]. Due to this simultaneous gamma-ray irradiation and heating, the soft epoxy resin becomes cured and cross-linked, which makes the resin harder by the formation of three-dimensional structures. Namely, at a relatively early stage of degradation, it seems that the cross-linking and curing dominantly occur in the rubber component added in the resin and the epoxy resin itself as well. The changes in T_{gl} observed in the samples concurrently aged by gamma rays at 100 °C should reflect the above mechanical and structural changes, although the oxidation follows if the penetration of oxygen is sufficient.

Here, T_{gl} of sample R is not so high even though the total dose of 800 kGy is high compared to 400 kGy finally given to the above concurrently aged sample used in the previous research [12]. Although not shown, the glass transition temperature of the present soft epoxy resin measured by DSC shows a drastic increase when it is aged purely thermally at temperatures from 90 °C to 120 °C without simultaneous irradiation of gamma rays. Since epoxy resin, not mentioning only the present soft one but epoxy resin in general, is thermoset, a high temperature would promote the elevation of the glass

transition temperature. For this reason, T_{gl} of sample R, which was not experienced a high temperature, does not go up so high. Figure 3 also indicates that all the samples other than P, R, and RS_m became as hard as the sample aged purely thermally for 2000 h or 4000 h. It also indicates that the steam exposure does not change the thermal property.

The real part E' and the imaginary part E'' of the complex elastic modulus shown in Figure 4 exhibit almost the same dependence on the aging time as T_{gl}. Therefore, it is reasonably assumed that the cross-linking and the resultant formation of three-dimensional structures and hardening are responsible for the above changes in the two moduli E' and E'', as in the case of T_{gl} mentioned above.

4.3. Mechanical Properties

Regarding the three mechanical properties—EAB, TS, and IM—we first pay attention to TS shown in Figure 5b. It is generally thought that TS should increase and decrease as the sample becomes harder and more brittle, respectively. That is, the results shown in Figure 5b reflect that, as already mentioned, the gamma-ray irradiation promotes the hardening of the sample associated with its cross-linking, while the steam exposure causes the embrittlement associated with the cleavage of chemical bonds. As a fact to discuss, TS becomes higher in sample RS_m than in R. Sample RS_m was exposed to the high temperature of 171 °C for the first time when exposed to water steam. The gamma-ray irradiation R should have generated many radicals in the sample R. If such a sample, in which radicals remain abundantly, is exposed to high temperature, cross-linking will occur vigorously. This seems to be the reason for the high TS in RS_m. The results of TS measured in the other steam-exposed samples indicate that the steam exposure promotes their embrittlement more severely by S_h than S_m.

The results of IM shown in Figure 6a are similar to those of TS shown in Figure 5b, except for the samples exposed to steam. The similarity between the two results is natural since both IM and TS measure the hardness of the sample, although there is a difference that TS reflects the hardness of the entire sample, while IM reflects that of the sample surface. The above explanation can be rephrased in detail, as will be mentioned below. When a sample becomes brittle, the entire one does not become brittle uniformly. Parts already embrittled and parts remaining hard should be mixed. A dumbbell-shaped sample should be broken at the most brittle part in a tensile test. Therefore, TS would decrease significantly even if only a tiny part of the sample becomes brittle. On the other hand, the average hardness of the sample surface under a pushing needle will be measured by IM. This means that IM reflects the hardening and embrittlement of the entire sample surface. Of course, if the mixture size of the brittle and hard parts exceeds that of the pushing needle on the surface, the variation of IM will increase when the number of measurement points on the surface increases. Figure 6b reflects this situation.

In contrast, the high IM values measured in the steam-exposed samples indicate that the steam exposure makes the samples brittle while keeping their surfaces hard. In addition, as indicated by comparing Figure 6a,b, when the IM values are high, they tend to scatter widely. It is reasonable statistically as mentioned above, but it also indicates that the steam exposure following the gamma-ray irradiation makes the surface mechanically inhomogeneous with mottled hard and brittle points.

It is indicated that EAB shown in Figure 5a decreases regardless of whether the sample became hard or brittle. Considering that the degradation of many polymers, especially rubbers not limited to this sample, progresses from hardening to embrittlement [14,18,20,33,38,39], EAB can be a suitable parameter as a degradation index. This view is also consistent with the above-mentioned assumption that sample RS_m was not damaged so much.

4.4. Dielectric Properties

Finally, regarding ε_r' and ε_r'' shown in Figure 7, their high values measured in sample P are most likely due to the rubber-based additive. For considering the mechanism un-

derlying such high values, the dependence of ε_r' and ε_r'' of sample P on the frequency of the voltage applied to the sample was measured. Figure 10 shows the frequency spectra of ε_r' and ε_r'' measured in sample P at room temperature around 20 °C. For comparison, frequency spectra of ε_r' and ε_r'' measured in conventional or ordinary hard bisphenol A epoxy resin are also shown. The discontinuity of the ε_r'' spectrum and the apparent loss peak appearing around 5 kHz in the hard epoxy resin are due to the frequency-range change of the measuring device. Both ε_r' and ε_r'' stay stable and low values in the hard epoxy resin. In marked contrast, they become drastically high in sample P with a decrease in frequency.

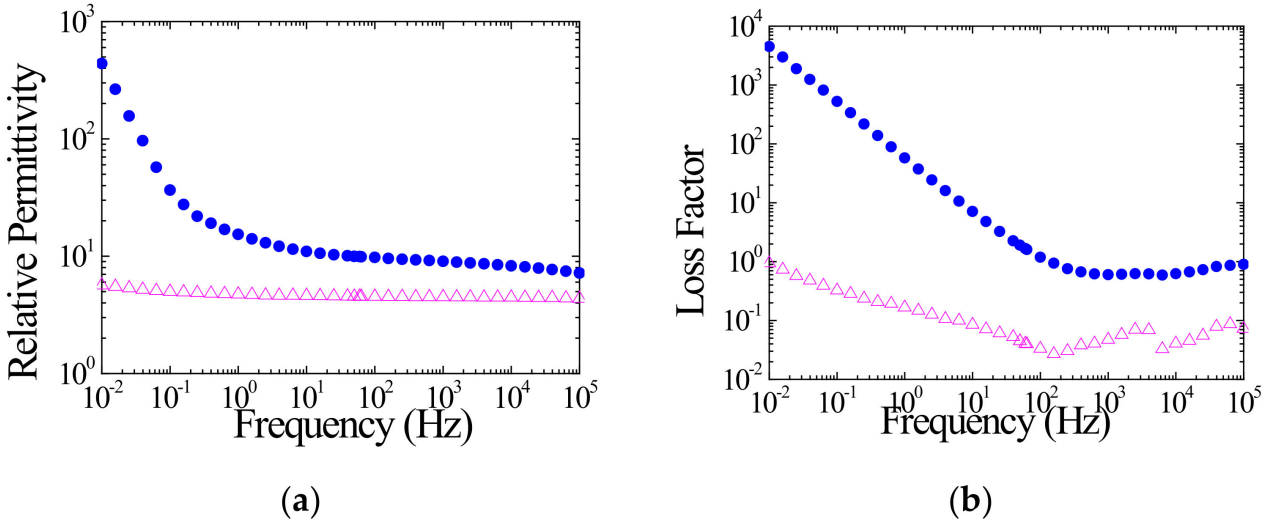


Figure 10. (**a**) ε_r' and (**b**) ε_r'' measured at 20 °C for sample P (•) and hard epoxy resin (Δ).

Another important feature is that ε_r'' in sample P increases in Figure 10 with a slope of −1 on the log–log graph with a decrease in frequency f in a relatively low frequency range from 10^{-2} to around 10 Hz. That is, the increment of ε_r'', $\Delta\varepsilon_r''$, satisfies Equation (1)

$$\Delta\varepsilon_r'' = \frac{\sigma}{2\pi f \varepsilon_0} \quad (1)$$

Here, σ is the conductivity. This indicates that $\Delta\varepsilon_r''$ is due to the Joule heating induced by the transport of charge carriers inside the sample [5–7,12,40]. In addition, if mobile carriers accumulate in front of electrodes, charge carriers with the polarities opposite to those of the mobile carriers must be supplied to the electrode(s) from an external power source. Therefore, ε_r' becomes higher accordingly. This is called electrode polarization [5,12,40]. Therefore, far more abundant mobile charge carriers—probably ionic [3,12]—are present in the soft epoxy resin than in the ordinary hard epoxy resin.

Regarding the above, Figure 7 indicates that the transport or movement of mobile carriers is hindered, resulting in the decrease in ε_r' and ε_r'' as the sample is degraded and becomes harder. The hindrance of the orientation of dipoles would also contribute to the decrease in ε_r' and ε_r''. A similar decrease in ε_r' and ε_r'' can be seen in other polymeric materials when aged thermally or by the irradiation of gamma rays [15,18,21]. On the other hand, the high values of ε_r' and ε_r'' measured in CRS_h indicate the aforementioned permeation of water steam into the sample under the high temperature of 200 °C and high pressure of 0.9 MPaG.

4.5. Comparison with Ordinary Epoxy Resin

It has become clear that the above various properties of the soft epoxy resin deteriorate dramatically due to its degradation, although its insulating property becomes improved since both ε_r' and ε_r'' decrease except when the steam penetrates the sample. It is thought

that the rubber-based additives contained in the resin are the main cause of these property changes. On the other hand, ordinary epoxy resin does not show such noticeable changes except when it receives extremely severe degradation, as reported in our previous paper [12]—although we did not examine the effects of steam exposure experimentally. Regarding the above, it cannot be denied that the soft epoxy resin is inferior to the ordinary epoxy resin in terms of stability against degradation caused by a severe accident. However, what is important here is that the characteristics of the aged soft epoxy resin approach or exceed the corresponding ones of the non-degraded ordinary epoxy resin, except for the extreme degradation, as far as the simultaneous aging with heat and gamma-ray irradiation previously reported [12] and purely thermal aging [41] are concerned. As a consequence, it can be said that there is no particular problem in using both resins according to their purposes unless they are so severely degraded.

5. Conclusions

Various properties and their changes induced by aging treatments were examined for the soft epoxy resin with rubber-based additives used for airtight sealing and electrical insulation in electrical penetrations in nuclear power plants.

(1) The epoxy resin has a low glass transition temperature, good flexibility, and a high dielectric constant, which seems to be due to the rubber-based additives.

(2) When the resin is aged by the exposure to heat, gamma-ray irradiation, and superheated water steam containing no oxygen, crosslinking, hardening, and embrittlement occur in the resin. The rubber-based additives seem to be mainly responsible for the above property changes. Especially in a relatively early stage of the degradation, the property changes of additives appear more distinctively than those of the epoxy resin component.

(3) The resin melts and disappears when it is directly exposed to water steam at either 171 °C or 200 °C.

(4) When the resin is irradiated with gamma rays at a high dose rate, cross-linking proceeds. This is because the occurrence of cross-linking becomes more active than oxidation when the diffusion of oxygen into the sample is not sufficient.

(5) The cross-linking slows down the molecular motions. Because of this, the glass transition temperature shifts toward higher temperatures. Both ε_r' and ε_r'' also decrease to bring about a better insulating property except when the steam penetrates the sample.

(6) Since the cross-linking hinders the penetration of water molecules into the sample, prior gamma-ray irradiation suppresses the embrittlement induced by the subsequent exposure to water steam. Namely, the hydrolysis induced by water steam can be mitigated by gamma-ray irradiation if it is properly conducted beforehand.

(7) Although the property changes induced in soft epoxy resin by the aging are drastic, its various properties observed resultantly are similar to the corresponding ones of the non-degraded ordinary hard epoxy resin. Therefore, it seems that using soft epoxy resin according to its purposes would not be a problem.

Author Contributions: Conceptualization, Y.O. and N.H.; methodology, N.H.; software, H.I.; validation, H.I. and N.H.; formal analysis, H.I. and N.H.; investigation, H.I.; resources, N.H.; data curation, H.I. and N.H.; writing—original draft preparation, H.I. and Y.O.; writing—review and editing, Y.O.; visualization, H.I. and N.H.; supervision, Y.O.; project administration, N.H.; funding acquisition, N.H. and Y.O. Ms. Mayu Hayashi, a former student supervised by Y.O., conducted parts of the experiments. The authors acknowledge her in Acknowledgments. All authors have read and agreed to the published version of the manuscript.

Funding: This research was performed under the research entrusted by the Secretariat of the Nuclear Regulation Authority in Japan.

Institutional Review Board Statement: Not applicable.

Informed Consent Statement: Not applicable.

Data Availability Statement: Not applicable.

Acknowledgments: The authors would like to thank Mayu Hayashi for sharing her experimental results.

Conflicts of Interest: The authors declare no conflict of interest.

References

1. Dakin, T.W. Application of epoxy resins in electrical apparatus. *IEEE Trans. Electr. Insul.* **1974**, *EI-9*, 121–128. [CrossRef]
2. Jin, F.L.; Li, X.; Park, S.J. Synthesis and application of epoxy resins: A review. *J. Ind. Eng. Chem.* **2015**, *29*, 1–11. [CrossRef]
3. Ulański, J.; Friedrich, K.; Boiteux, G.; Seytre, G. Evolution of ion mobility in cured epoxy-amine system as determined by time-of-flight method. *J. Appl. Polym. Sci.* **1997**, *65*, 1143–1150. [CrossRef]
4. Ohki, Y. Development of a high-performance casting method for solid-insulated switchgear [News from Japan]. *IEEE Electr. Insul. Mag.* **2010**, *26*, 63–65. [CrossRef]
5. Tian, F.; Ohki, Y. Charge Transport and Electrode Polarization in Epoxy Resin at High Temperatures. *J. Phys. D Appl. Phys.* **2014**, *47*, 1–9. [CrossRef]
6. Li, X.; Masuzaki, Y.; Tian, F.; Ohki, Y. Space Charge Formation and Charge Transport in Epoxy Resin at Varied Temperatures. *IEEJ Trans. Fundam. Mater.* **2015**, *135*, 88–93. [CrossRef]
7. Nagase, E.; Iizuka, T.; Tatsumi, K.; Hirai, N.; Ohki, Y.; Yoshida, S.; Umemoto, T.; Muto, H. Filler-dependent Changes in Thermal, Dielectric, and Mechanical Properties of Epoxy Resin Nanocomposites. *IEEJ Trans. Electr. Electron. Eng.* **2020**, *16*, 15–20. [CrossRef]
8. Umemoto, T.; Yoshida, S.; Muto, H.; Kurimoto, M. Critical Agglomerate Size for Electrical Insulation Lifetime Extension of Epoxy/TiO_2 Nanocomposite with a Void Defect. *IEEE Trans. Dielectr. Electr. Insul.* **2021**, *28*, 282–289. [CrossRef]
9. Clauss, D.B. Severe accident testing of electrical penetration assemblies. *NUREG/CR-5334* **1989**, 1–213. [CrossRef]
10. Mazzoni, O.S. 5. Nuclear plants containment electrical penetration assemblies. In *Electrical Systems for Nuclear Power Plants*, 1st ed.; Hossain, E., Fortino, G., Molisch, A., Shafer, L., Grier, D.A., Nahavandi, S., Shahidehpour, M., Heirman, D., Perez, R., Spurgeon, S., et al., Eds.; IEEE Press: Piscataway, NJ, USA, 2019; pp. 53–69.
11. Minakawa, T.; Watanabe, A.; Ikeda, M.; Taguchi, K. Study on long-term integrity of polymer materials for electrical equipment, Regulatory Standard and Research Department, Secretariat of Nuclear Regulation Authority, Japan, 2020, RREP-2020–1001, pp. 4–39. (In Japanese).
12. Ishii, H.; Hirai, N.; Ohki, Y. Comparison of degradation behavior between soft and hard epoxy resins. *J. Nucl. Sci. Technol.* **2020**, *58*, 620–628. [CrossRef]
13. Zhou, H.; Hirai, N.; Ohki, Y. Various characteristics of severely aged flame-retardant cross-linked polyolefin. *IEEJ Trans. Electr. Electron. Eng.* **2021**, *16*, 1–7. [CrossRef]
14. Ito, S.; Miyazaki, Y.; Hirai, N.; Ohki, Y. Effects of gamma irradiation on the degradation of silicone rubber by steam exposure. *J. Nucl. Sci. Technol.* **2021**, *58*, 166–172. [CrossRef]
15. Zhou, H.; Hanafusa, W.; Udo, K.; Hirai, N.; Ohki, Y. Aging behavior of flame-retardant cross-linked polyolefin under thermal and radiation stresses. *IEEE Trans. Dielectr. Electr. Insul.* **2021**, *28*, 303–309. [CrossRef]
16. Miyazaki, Y.; Hirai, N.; Ohki, Y. Effects of heat and gamma-rays on mechanical and dielectric properties of cross-linked polyethylene. *IEEE Trans. Dielectr. Electr. Insul.* **2020**, *27*, 1998–2006. [CrossRef]
17. Yamaguchi, H.; Ishii, H.; Hirai, N.; Ohki, Y. Degradation of mechanical and dielectric properties of flame-retardant ethylene propylene rubber by thermal aging. *IEEJ Trans. Electr. Electron. Eng.* **2020**, *15*, 488–495. [CrossRef]
18. You, J.; Yamaguchi, H.; Ishii, H.; Hirai, N.; Ohki, Y. Degradation of flame-retardant ethylene-propylene-diene rubber by radiation and steam. *IEEJ Trans. Electr. Electron. Eng.* **2020**, *15*, 1572–1579. [CrossRef]
19. Liu, Z.; Miyazaki, Y.; Hirai, N.; Ohki, Y. Comparison of the effects of heat and gamma irradiation on the degradation of cross-linked polyethylene. *IEEJ Trans. Electr. Electron. Eng.* **2020**, *15*, 24–29. [CrossRef]
20. Kaneko, T.; Ito, S.; Minakawa, T.; Hirai, N.; Ohki, Y. Degradation mechanisms of silicone rubber under different aging conditions. *Polym. Degrad. Stab.* **2019**, *168*, 108936. [CrossRef]
21. Yang, Z.; Kaneko, T.; Hirai, N.; Ohki, Y. Aging behavior of flame-retardant cross-linked polyethylene in nuclear power plant environments. *IEEJ Trans. Electr. Electron. Eng.* **2019**, *14*, 1133–1138. [CrossRef]
22. Liu, S.; Fifield, L.S.; Bowler, N. Aging mechanisms of filled cross-linked polyethylene (XLPE) cable insulation material exposed to simultaneous thermal and gamma radiation. *Radiat. Phys. Chem.* **2021**, *185*, 1–9. [CrossRef]
23. Spencer, M.P.; Zwoster, A.; Bisel, T.T.; Murphy, M.K.; Fifield, L.S. Sequential versus simultaneous aging of XLPE nuclear cable insulation subjected to elevated temperature and gamma radiation. In Proceedings of the IEEE Electrical Insulation Conference 2020, Knoxville, TN, USA, 22 June–3 July 2020; pp. 50–53. [CrossRef]
24. Suraci, S.V.; Fabiani, D. Aging modeling of low-voltage cables subjected to radio-chemical aging. *IEEE Access* **2021**, *9*, 83569–83578. [CrossRef]
25. Suraci, S.V.; Fabiani, D.; Mazzocchetti, L.; Giorgini, L. Degradation Assessment of Polyethylene-Based Material Through Electrical and Chemical-Physical Analyses. *Energies* **2020**, *13*, 650. [CrossRef]
26. Available online: https://www.team-cables.eu/ (accessed on 9 October 2021).
27. Japan Nuclear Energy Safety Organization The final report of the project of "assessment of cable aging for nuclear power plants", JNES-SS-0903; 2009.
28. Japan Nuclear Energy Safety Organization Report on assessment of electrical equipment aging for nuclear power plant (AEA), FY2012, JNES-RE-2013–0016; 2013. (In Japanese)

29. Regulatory Standard and Research Department, Secretariat of Nuclear Regulation Authority Analysis of insulation performance of cables under severe accident environmental conditions, NTEC-2019–1002; 2019. (In Japanese)
30. Regulatory Standard and Research Department, Secretariat of Nuclear Regulation Authority Study on long-term integrity of polymer materials for electrical equipment, RREP-2020–1001; 2020. (In Japanese)
31. Japanese Standards Association, Plastics-Determination of Dynamic Mechanical Properties-Part 4: Tensile Vibration-Non-resonance Method, JIS K 7244–4:1999; 1999. (In Japanese)
32. Japanese Standards Association Plastics-Test specimens; JIS K 7139:2009, 2009. (In Japanese)
33. IEC/IEEE 62582–2: 2011/AMD1: Nuclear Power Plants-Instrumentation and Control Important to Safety-Electrical Equipment Condition Monitoring Methods—Part 2: Indenter Modulus; 2016.
34. Jones, D.S. Dynamic mechanical analysis of polymeric systems of pharmaceutical and biomedical significance. *Int. J. Pharm.* **1999**, *179*, 167–178. [CrossRef]
35. Achorn, P.J.; Ferrillo, R.G. Comparison of thermal techniques for glass transition measurements of polystyrene and cross-linked acrylic polyurethane films. *J. Appl. Polym. Sci.* **1994**, *54*, 2033–2043. [CrossRef]
36. Arakawa, K.; Seguchi, T.; Watanabe, Y.; Hayakawa, N.; Kuriyama, I.; Machi, S. Dose rate effect on radiation-induced oxidation of polyethylene and ethylene-propylene copolymer. *J. Polym. Sci. Polym. Chem. Ed.* **1981**, *19*, 2123–2125. [CrossRef]
37. Hanisch, F.; Maier, P.; Okada, S.; Schönbacher, H. Effects of radiation types and dose rates on selected cable-insulating materials. *Int. J. Radiat. Appl. Instrum. Part C. Radiat. Phys. Chem.* **1987**, *30*, 1–9. [CrossRef]
38. Deepalaxmi, R.; Rajini, V. Performance evaluation of gamma irradiated SiR-EPDM blends. *Nucl. Eng. Des.* **2014**, *273*, 602–614. [CrossRef]
39. Fuse, N.; Misaka, H.; Homma, H.; Okamoto, T. Mechanism elucidation of degradation dynamics of ethylene propylene rubber cable insulations sampled from nuclear power containment using additional aging. *IEEE Trans. Dielectr. Electr. Insul.* **2016**, *23*, 730–737. [CrossRef]
40. Ohki, Y.; Hirai, N. Effects of resin/filler adhesion on the thermal and electrical conductivity of polyimide nanocomposites. *J. Compos. Sci.* **2021**, *5*, 272. [CrossRef]
41. Tsutsui, J.; Shimizu, A.; Hayashi, M.; Ishii, H.; Ohki, Y.; Hirai, N. Various properties of thermally aged hard and soft epoxy resins. Joint Technical Meeting on Dielectrics and Electrical Insulation and Electric Wire and Power Cable, Online, 12 March 2021; Inst. Electr. Eng. Japan, Tokyo, Japan, 2021; DEI-21-063; pp. 77–82. (In Japanese)